Supplementary Information:

Geochemistry of PM10 over Europe during the EMEP intensive measurement periods in summer 2012 and winter 2013

Andrés Alastuey[1], Xavier Querol[1], Wenche Aas[2], Franco Lucarelli[3], Noemí Pérez[1], Teresa Moreno[1], Fabrizia Cavalli[4], Hans Areskoug[5], Violeta Balan[6], Maria Catrambone[7], Darius Ceburnis[8], José C. Cerro[9], Sébastien Conil[10], Lusine Gevorgyan[11], Christoph Hueglin[12], Kornelia Imre[13], Jean-Luc Jaffrezo[14], Sarah R. Leeson[15], Nikolaos Mihalopoulos[16], Marta Mitosinkova[17], Jorge Pey[18], Jean-Philippe Putaud[6], Véronique Riffault[19], Anna Ripoll[1], Jean Sciare[20, 21], Karine Sellegri[22], Gerald Spindler[23], Karl Espen Yttri[2]

[1] Institute of Environmental Assessment and Water Research (IDAEA-CSIC), Barcelona, Spain
[2] NILU-Norwegian Institute for Air Research, Kjeller, Norway
[3] Dipartimento di Fisica e Astronomia and National Institute of Nuclear Physics (INFN), Sesto Fiorentino (Firenze), Italy
[4] European Commission – DG Joint Research Centre, Ispra, Italy
[5] Stockholm University, ACES, Stockholm, Sweden
[6] Hydrometeorologic State Service, Ministry of Ecology and Natural Resources, Chisinau, Moldova
[7] CNR, Institute of Atmospheric Pollution Research, Monterotondo Stazione (Rome), Italy
[8] School of Physics, National University of Ireland Galway, Galway, Ireland
[9] Laboratory of Environmental Analytical Chemistry, Illes Balears University, Spain
[10] ANDRA - DRD - Observation Surveillance, Observatoire Pérenne de l'Environnement, Bure, France
[11] Environmental Impact Monitoring Center, Yerevan, Armenia
[12] Empa, Swiss Federal Laboratories for Materials Science and Technology 8600 Dübendorf, Switzerland
[13] MTA-PE Air Chemistry Research Group, University of Veszprém, Veszprém, Hungary
[14] Laboratoire de Glaciologie et Géophysique de l'Environnement, UGA-CNRS, St Martin d'Hères Cedex, France
[15] Centre for Ecology and Hydrology (CEH), Bush Estate EH26 0QB, UK
[16] Environmental Chemical Processes Laboratory, University of Crete, Heraklion, Greece
[17] Slovak Hydrometeorological Institute, Bratislava, Slovak Republic
[18] Spanish Geological Survey. Zaragoza IGME Unit, Zaragoza, Spain
[19] Département Sciences de l'Atmosphère et Génie de l'Environnement (SAGE), Mines Douai, Douai, France
[20] Laboratoire des Sciences du Climat et de l'Environnment, Gif/Yvette, France
[21] The Cyprus Institute, Energy, Environment and Water Research Center, Nicosia, Cyprus
[22] Laboratoire de Météorologie Physique LaMP-CNRS/OPGC, Aubiere, France
[23] Leibniz Institute for Tropospheric Research (TROPOS) Leipzig, Germany

Correspondence to: Andrés Alastuey (andres.alastuey@idaea.csic.es)

Table S1: Average minimum detection limit (MDL) for the elements measured.

MDL					
	ng/cm^2	ng/m^3		ng/cm^2	ng/m^3
Na	24.8	5.5	**Ti**	4.8	1.1
Mg	18.9	4.2	**V**	3.4	0.7
Al	12.7	2.8	**Cr**	2.1	0.5
Si	10.2	2.3	**Mn**	1.5	0.3
P	9.3	2.0	**Ni**	0.6	0.1
S	9.9	2.2	**Cu**	0.6	0.1
Cl	11.1	2.5	**Zn**	0.6	0.1
K	11.5	2.5	**As**	0.8	0.2
Ca	9.2	2.0	**Se**	0.9	0.2
Fe	1.1	0.2	**Br**	1.2	0.3
			Rb	1.9	0.4
			Sr	2.5	0.5
			Zr	4.0	0.9
			Mo	7.4	1.6
			Ba	12.8	2.8
			Pb	1.7	0.4

Table S2. Slope and R2 determination coefficients for concentrations determined by PIXE and ICPs (PIXE = a * ICPs) at ES1778. n= number of data pairs available for the correlation.

	ICPs ES1778					
		y=ax		y=ax + b		
	n	slope	R^2	slope	constant	R^2
Al	38	1.02	0.99			
Fe	38	1.04	0.99			
K	38	1.03	0.97			
Mg	38	1.26	0.97			
Ca	38	1.05	0.95			
S	38	1.01	0.93			
Na	38	1.13	0.91			
Si	--	--	--	--	--	--
Ti	37	1.22	0.98			
Mn	34	1.03	0.98			
Zn	38	1.04	0.81	0.90	2.18	0.84
Cu	37	1.11	0.71	0.89	0.75	0.76
V	26	1.29	0.49	0.93	2.19	0.63
Pb	11	0.94	0.40	0.63	1.37	0.60
Cr	21	1.64	-0.72	0.81	2.60	0.69
Sr	12	0.77	-2.01	0.30	3.39	0.65
Ni	35	1.14	-0.44	0.48	1.58	0.19
Cl	38	0.62	0.31	0.69	2.93	0.32

Table S3. Mean concentrations of PM10, major (µg m-3) and trace elements (ng m-3) during the summer 2012 IMP.

Summer	AM01	CH02	DE44	GR02	IT04	MD13	SE12	SK06	GB48	IT01	ES778	FR30	HU02	ESCLl	IE31	FR22	FR09	ES22
N	**32**	**40**	**37**	**39**	**37**	**44**	**26**	**32**	**32**	**39**	**41**	**22**	**39**	**17**	**31**	**7**	**7**	**28**
µg m^{-3}																		
PM_{10}	14.0	12.3	20.0	25.0	14.8	26.2	7.7	15.2	4.5	31.1	27.50	2.9	15.3	18.1	12.9	--	13.6	21.0
Na	0.06	0.11	0.14	1.30	0.20	0.11	0.36	0.08	0.22	0.80	0.70	0.04	0.02	0.93	0.77	0.27	0.37	0.33
Mg	0.23	0.05	0.05	0.28	0.09	0.21	0.06	0.07	0.04	0.23	0.23	0.02	0.09	0.25	0.12	0.13	0.10	0.18
Al	0.50	0.15	0.13	0.39	0.23	0.87	0.04	0.28	0.03	0.62	0.61	0.07	0.37	0.31	0.04	0.45	0.25	0.73
Si	1.32	0.37	0.30	0.97	0.59	2.46	0.10	0.67	0.08	1.34	1.29	0.16	--	0.72	0.04	0.95	0.51	--
Ca	0.69	0.18	0.08	0.44	0.16	0.77	0.04	0.14	0.03	1.42	0.52	0.03	0.35	0.64	0.04	0.31	0.15	0.68
Fe	0.29	0.13	0.11	0.30	0.26	0.62	0.04	0.19	0.03	0.48	0.36	0.03	0.23	0.22	0.01	0.25	0.15	0.40
S	0.76	0.36	0.66	1.97	0.85	1.12	0.53	0.88	0.37	1.15	0.92	0.17	0.66	0.72	0.39	0.60	0.58	0.59
Cl	0.02	0.03	0.04	1.05	0.02	0.02	0.08	0.01	0.15	0.39	0.17	<0.1	-	0.80	1.12	0.10	0.16	0.09
K	0.19	0.12	0.12	0.25	0.14	0.44	0.06	0.17	0.04	0.35	0.23	0.03	0.09	0.17	0.04	0.18	0.11	0.17
ng m^{-3}																		
P	3.8	23.4	31.0	3.2	7.5	14.1	7.6	21.5	5.8	9.6	11.1	0.8	<0.5	11.8	4.7	26.9	13.3	17.9
Ti	31.7	9.9	8.3	27.2	14.6	56.3	3.0	18.9	2.9	36.3	42.8	4.8	22.8	21.5	3.0	29.0	15.2	48.8
V	0.5	0.7	1.1	6.2	1.7	1.9	1.0	1.0	0.9	4.8	4.8	0.2	1.0	3.9	1.4	2.2	1.7	2.8
Cr	1.3	1.0	1.6	1.1	1.1	2.2	0.3	4.4	0.6	2.6	2.8	0.2	1.8	2.3	1.1	1.3	1.1	1.3
Mn	9.0	2.8	3.0	6.8	4.2	16.9	1.2	4.6	0.9	9.8	6.9	0.9	7.0	4.2	0.8	5.5	3.6	9.9
Ni	1.1	0.5	0.8	2.5	1.3	1.1	0.9	2.1	0.6	2.2	2.1	0.2	3.3	1.7	0.6	254	150	1.1
Cu	1.3	2.8	2.7	2.0	8.3	2.5	0.8	2.4	0.8	11.1	3.4	0.5	4.0	2.9	0.7	0.6	0.5	2.0
Zn	12.4	7.5	14.3	21.9	14.4	18.0	4.5	19.7	8.2	18.9	14.5	5.4	7.3	7.4	12.0	2.4	1.8	6.4
As	1.6	0.2	0.6	0.6	0.2	0.6	0.3	0.7	0.3	0.1	0.8	0.1	0.5	0.7	0.3	17.2	20.1	0.2
Se	0.6	0.2	0.6	0.6	0.4	1.1	0.2	0.5	0.3	0.5	1.1	0.0	0.3	0.9	0.4	0.6	0.5	0.3
Br	2.4	1.4	2.3	8.4	2.8	3.3	1.9	1.8	1.3	5.0	3.4	0.5	<0.5	4.9	3.3	0.6	0.8	<0.5
Rb	1.7	0.8	0.6	1.3	0.9	3.0	0.2	0.9	0.4	4.1	2.7	-	0.4	2.1	0.8	2.2	1.9	0.8
Sr	2.3	0.6	0.9	2.8	4.2	3.5	0.4	1.1	0.5	6.0	3.3	0.2	1.1	3.5	1.2	1.2	1.1	3.7
Zr	1.1	0.7	1.2	1.4	1.1	2.0	0.5	1.2	0.8	2.3	5.1	0.1	8.8	5.0	1.8	1.7	1.3	4.9
Mo	2.3	0.9	2.1	2.1	1.5	2.3	0.9	2.1	1.5	0.2	8.7	<0.2	7.0	7.8	3.2	2.2	2.1	<0.2
Ba	3.1	1.8	3.5	4.4	16.0	6.5	1.6	4.1	2.4	7.4	0.0	<0.2	3.8	8.1	5.1	4.0	3.7	5.0
Pb	7.5	1.2	2.3	15.2	3.8	5.8	1.2	2.4	0.9	4.1	2.1	0.2	2.7	1.9	0.8	9.2	7.3	1.6

Table S4. Mean concentrations of PM10, major (µg m-3) and trace elements (ng m-3) during the winter 2013 IMP.

Winter	CH02	DE44	GR02	IT04	MD13	SE12	SK06	GB48	IT01	ES1778	FR30	HU02	IE31	FR22	FR09	FR20	GB36	ES22
N	**29**	**28**	**30**	**29**	**29**	**29**	**29**	**20**	**29**	**31**	**12**	**26**	**14**	**9**	**6**	**8**	**26**	**22**
µg m^{-3}																		
PM_{10}	16.1	28.1	39.7	37.4	28.6	6.8	17.7	7.5	23.6	9.2	--	20.3	35.7	20.5	25.4	--	17.9	3.4
Na	0.18	0.31	1.51	0.21	0.13	0.34	0.10	0.91	0.57	0.20	0.01	0.49	6.10	0.38	0.28	0.40	1.00	0.06
Mg	0.03	0.06	0.76	0.05	0.05	0.06	0.02	0.15	0.13	0.05	0.01	0.03	1.00	0.07	0.06	0.07	0.17	0.01
Al	0.02	0.07	1.09	0.09	0.10	0.01	0.04	0.02	0.09	0.08	0.02	0.12	0.12	0.02	0.03	0.04	0.02	0.02
Si	0.08	0.14	2.55	0.23	0.25	0.04	0.09	0.04	0.20	0.17	0.04	--	0.04	0.06	0.07	0.12	0.06	--
Ca	0.08	0.07	2.37	0.16	0.09	0.03	0.07	0.04	0.25	0.09	0.01	0.07	0.25	0.06	0.07	0.11	0.07	0.05
Fe	0.08	0.07	0.67	0.42	0.12	0.03	0.05	0.02	0.15	0.05	0.01	0.02	0.01	0.07	0.10	0.20	0.08	0.01
S	0.47	1.18	0.58	0.66	1.27	0.46	1.23	0.28	0.41	0.15	0.05	0.81	0.55	0.99	1.24	0.89	0.67	0.05
Cl	0.21	0.31	2.18	0.40	0.18	0.19	0.01	1.06	0.54	0.08	<0.1	-	11.2	0.32	0.37	0.53	1.14	0.10
K	0.20	0.15	0.44	0.57	0.32	0.08	0.24	0.05	0.39	0.08	0.01	0.22	0.25	0.14	0.12	0.17	0.10	0.03
ng m^{-3}																		
P	7.3	3.2	5.8	4.2	1.5	1.1	2.8	1.7	3.3	2.8	1.2	<0.5	6.2	2.2	2.5	2.4	2.1	<0.5
Ti	2.1	4.8	69.6	7.1	6.7	1.0	2.7	1.4	5.7	4.7	0.6	2.8	2.8	1.7	3.2	3.9	2.0	3.6
V	0.4	1.1	3.4	0.9	1.0	0.5	1.0	0.7	1.0	1.0	0.5	0.4	1.9	0.7	1.2	1.2	1.0	0.1
Cr	0.9	0.8	1.7	2.7	0.5	0.3	1.2	0.4	3.7	0.7	0.3	1.3	1.7	1.1	2.0	1.8	0.8	1.2
Mn	2.3	2.7	10.0	6.6	3.5	1.5	2.2	0.5	3.3	2.3	0.2	1.1	1.0	3.6	5.2	4.6	1.7	0.8
Ni	0.3	0.7	1.2	1.9	0.7	0.5	0.8	0.4	2.1	0.4	0.2	0.8	0.8	0.7	1.0	1.1	0.7	0.1
Cu	3.6	3.3	1.4	15.9	2.3	0.9	2.2	0.9	5.7	2.3	0.5	0.1	1.0	2.3	3.2	9.4	3.4	0.3
Zn	17.9	35.7	19.0	36.0	24.5	15.0	27.7	9.9	18.4	14.4	5.1	11.4	16.4	37.5	59.1	40.9	22.9	3.0
As	0.3	1.3	0.6	0.7	1.2	0.4	0.8	0.4	0.3	0.3	0.1	1.2	0.5	0.4	0.7	0.6	0.9	0.1
Se	0.3	0.6	0.6	0.7	0.6	0.2	0.4	0.2	0.3	0.2	0.1	0.3	0.7	1.0	1.1	0.9	0.5	<0.2
Br	2.0	5.2	8.7	5.0	5.2	2.1	3.3	2.8	5.4	1.6	0.2	<0.2	28.6	3.3	5.1	6.1	5.6	<0.2
Rb	0.8	0.6	4.2	3.1	1.3	0.3	0.7	0.4	2.8	0.5	0.2	0.5	1.5	0.7	0.6	1.5	0.4	<0.2
Sr	0.4	0.8	8.5	16.3	0.8	0.4	0.7	0.8	1.6	0.7	0.3	0.4	5.6	0.7	0.7	0.9	1.0	0.2
Zr	0.6	1.0	3.5	1.5	0.7	0.5	1.0	0.8	1.1	0.9	0.5	11.0	2.9	1.1	1.1	1.6	0.9	0.4
Mo	0.9	1.7	3.1	2.1	1.0	0.9	1.8	1.4	1.1	1.7	1.0	3.0	5.2	1.7	1.9	1.7	1.5	<0.2
Ba	2.0	3.8	14.8	31.8	2.3	1.5	3.9	2.3	3.4	3.6	1.5	0.8	7.8	3.7	3.3	5.1	3.5	0.9
Pb	3.7	9.9	15.0	10.7	9.6	1.5	6.9	0.9	5.3	1.4	0.5	6.0	1.1	7.2	6.9	12.0	6.5	0.2

Figure

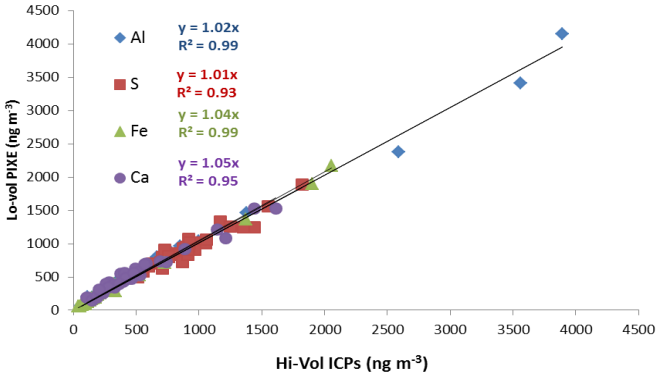

Figure S1: Correlation between concentrations of major elements determined by PIXE and ICPs at MSY (ES1778).

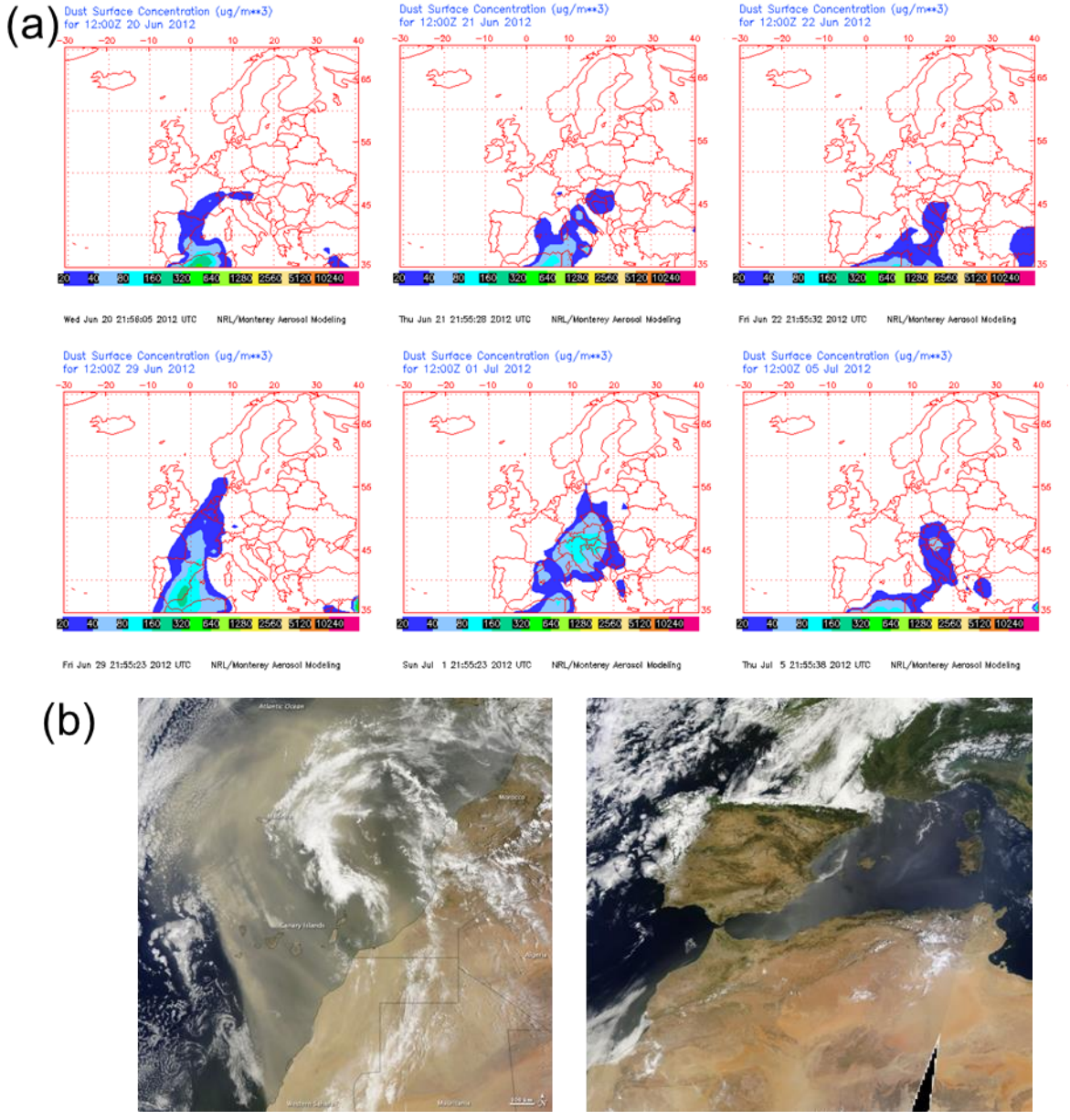

Figure S2: Two major dust episodes were observed in June/July 2012. For both cases, the dust outbreak was transported eastwards. As shown by: (a) dust surface concentration maps by NAAPS Navy Aerosol Analysis Prediction System from the Marine Meteorology Division of the Naval research Laboratory, USA (NRL) for June 20, 21, 22, 29 and July 01 and 05; (b) NASA Terra – MODIS, images courtesy MODIS Rapid Response Team, Goddard Space Flight Centre. Left: 2012/06/25. Right: 2012/06/30.

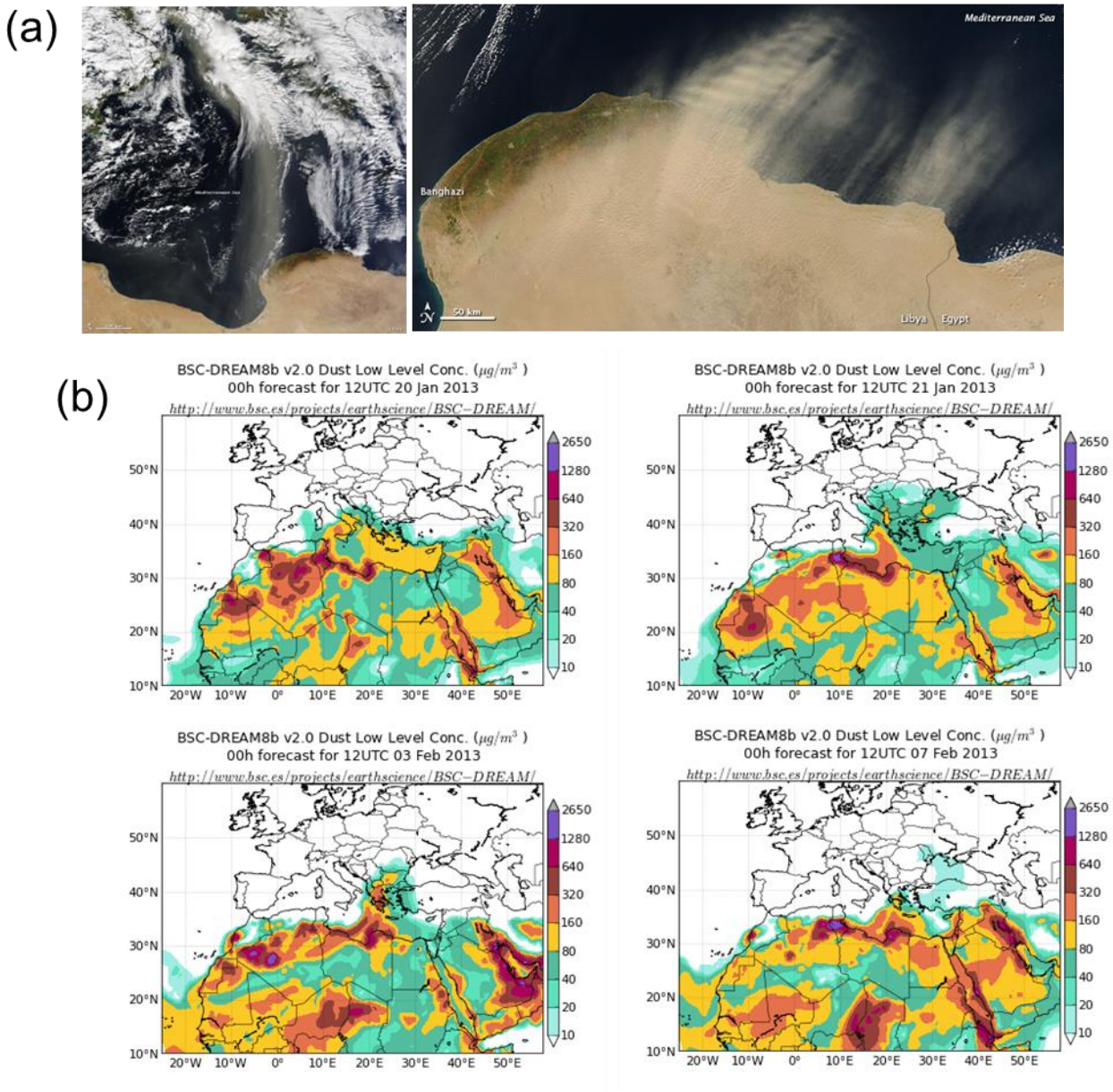

Figure S3: During the winter IMP, the eastern region was affected by short but intense pulses of dust. (a) Satellite images courtesy MODIS Rapid Response Team, Goddard Space Flight Center. Left: Terra – MODIS, 2013/01/21. Right: Aqua – MODIS Multiple dust plumes 2013/02/07 moving off the coast of Libya toward the northeast. (b) Maps of dust surface concentration from the BSC-DREAM8b (Dust REgional Atmospheric Model) model, operated by the Barcelona Supercomputing Center (BSC) for January 20 and 21 and February 03 and 07.

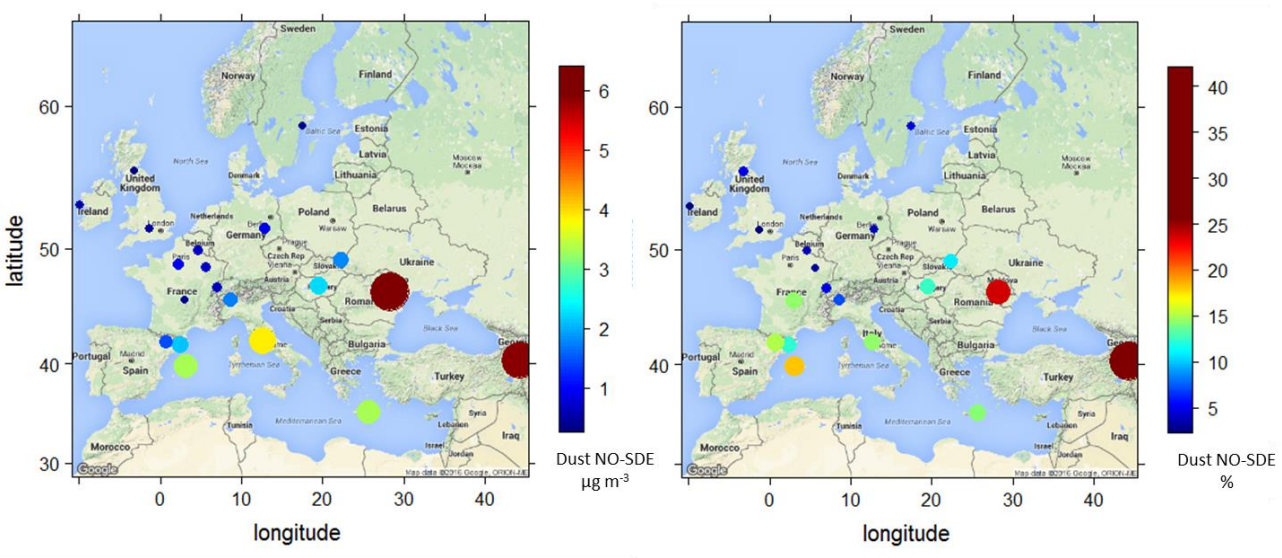

Figure S4: Spatial distribution of the average mineral dust concentration (µg m^{-3}) and its relative contribution (%) to PM_{10} obtained at each site in the summer 2012 and the winter 2013 IMPs during the Non-Saharan dust events (NO-SDE). The diameter of the circles is proportional to the concentrations.

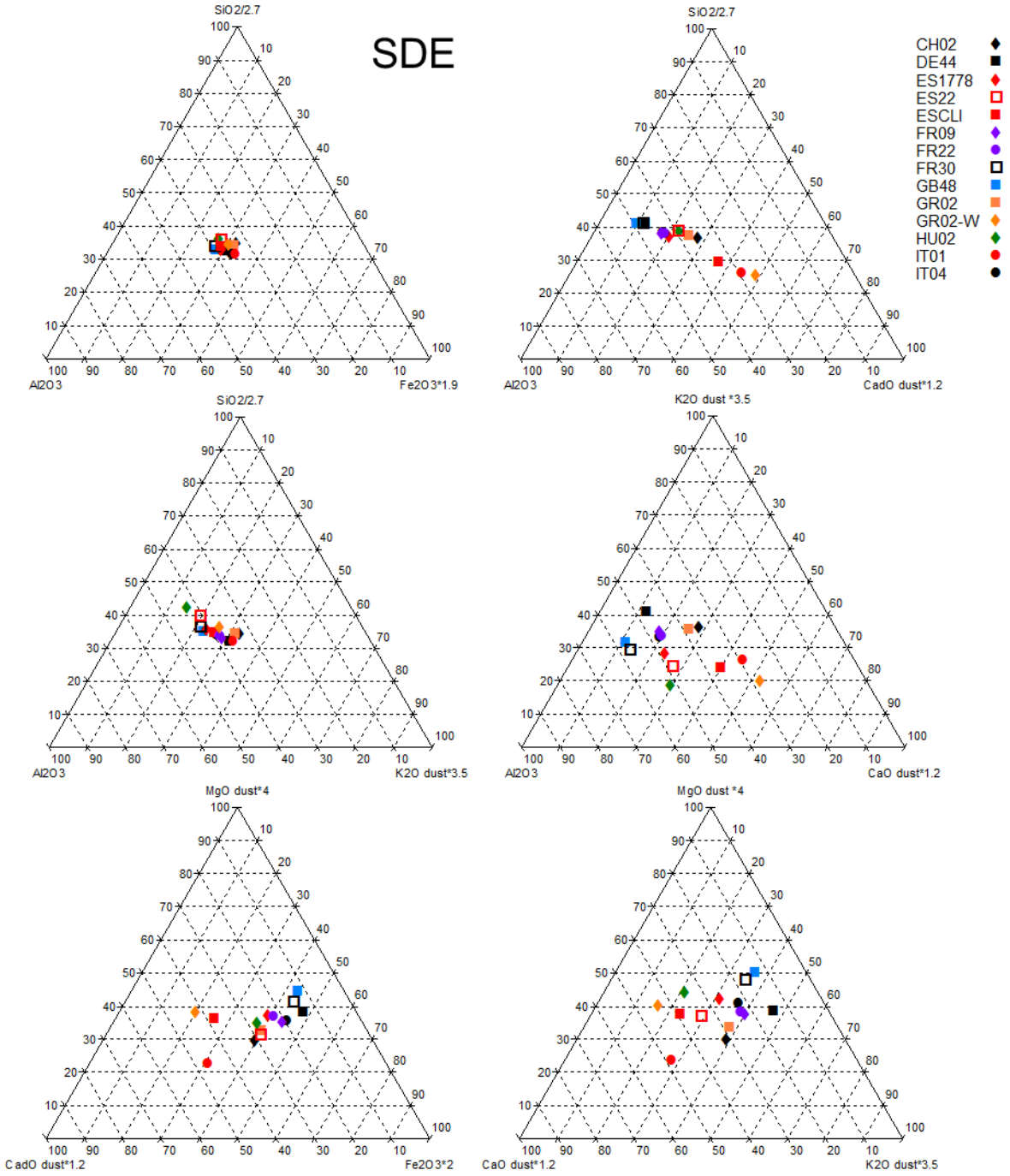

Figure S5: Ternary diagrams for major mineral components for days with Saharan dust impact (SDE). Orange: GR02; red: south-western and south central sites; purple: Central Western Europe; black: CE sites; blue: northern and Atlantic sites; green: eastern sites; empty symbol: high altitude sites.

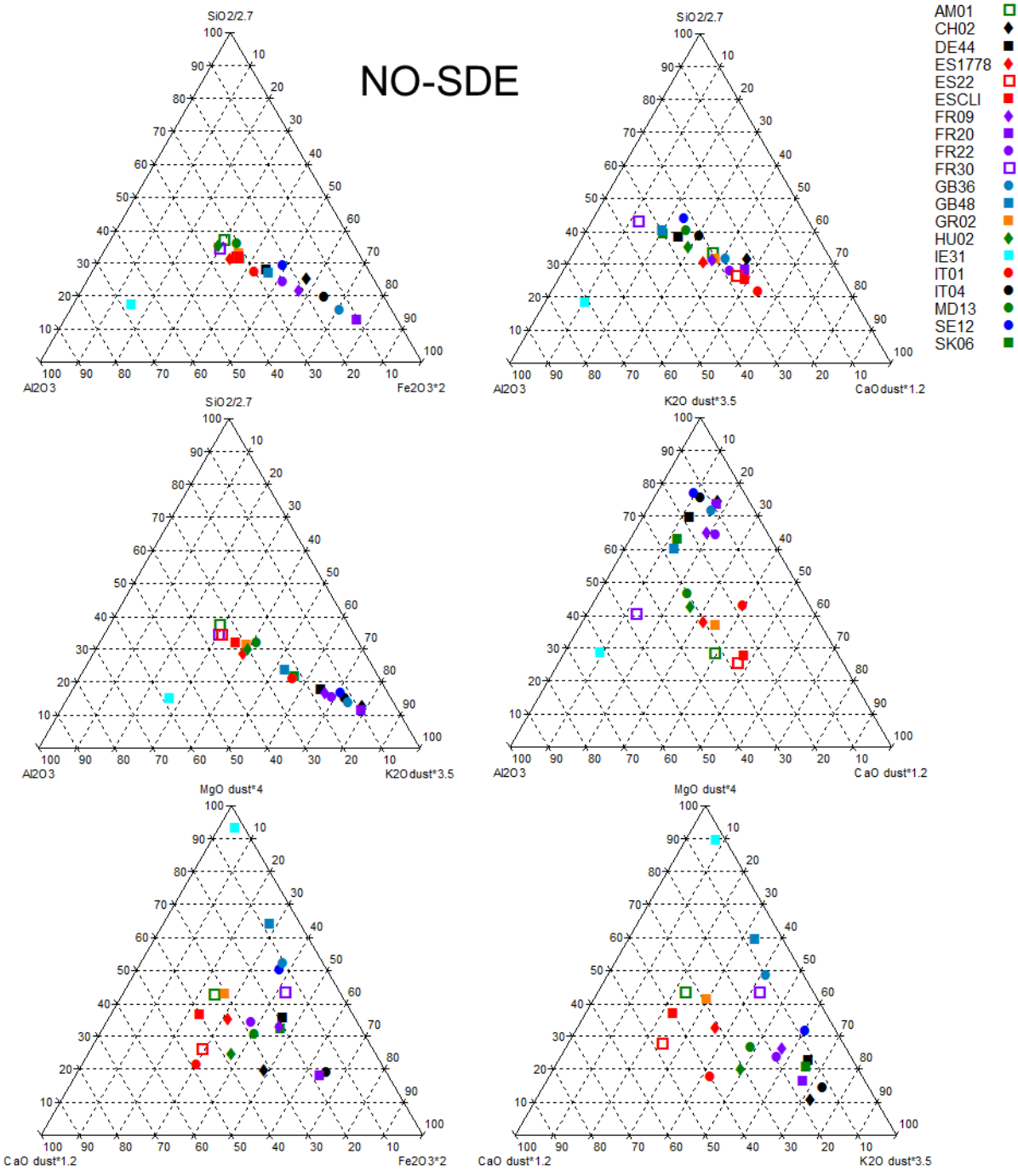

Figure S6: Ternary diagrams for average concentration (considering the two IMPs) of mineral dust major components for days without impact of Saharan dust (NO-SDE). Orange: GR02; red: south- western and south-central sites; purple: Central Western Europe; black: CE sites; blue; northern and Atlantic sites; green: eastern sites; empty symbols: high altitude sites.

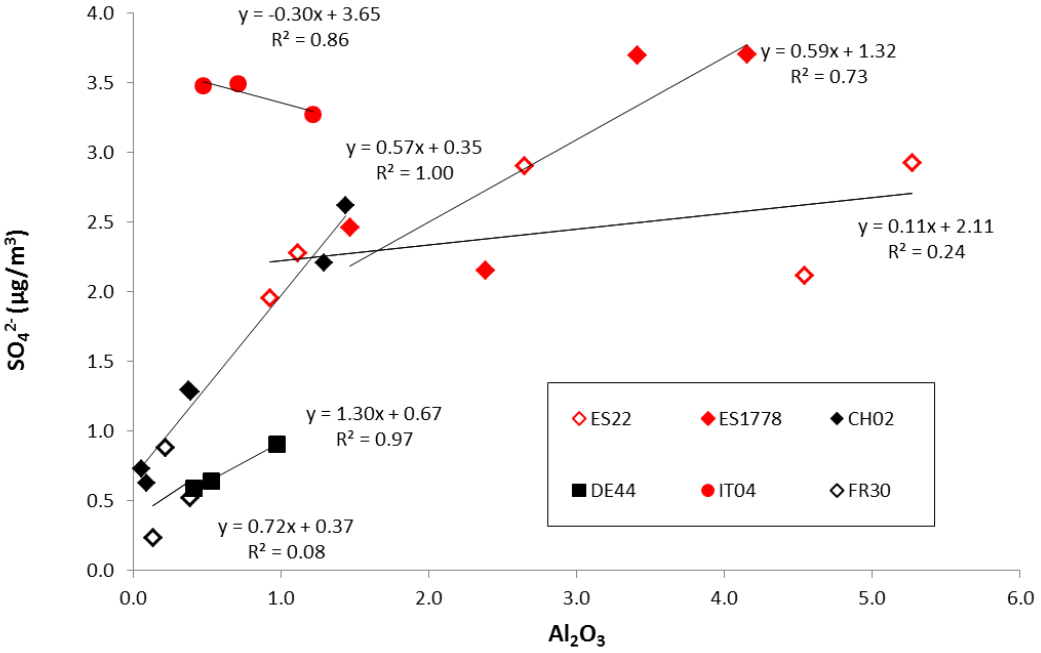

Figure S7: Correlation among daily concentrations of Al_2O_3 and SO_4^{2-} measured during Saharan dust outbreaks at different sites during the summer IMP.

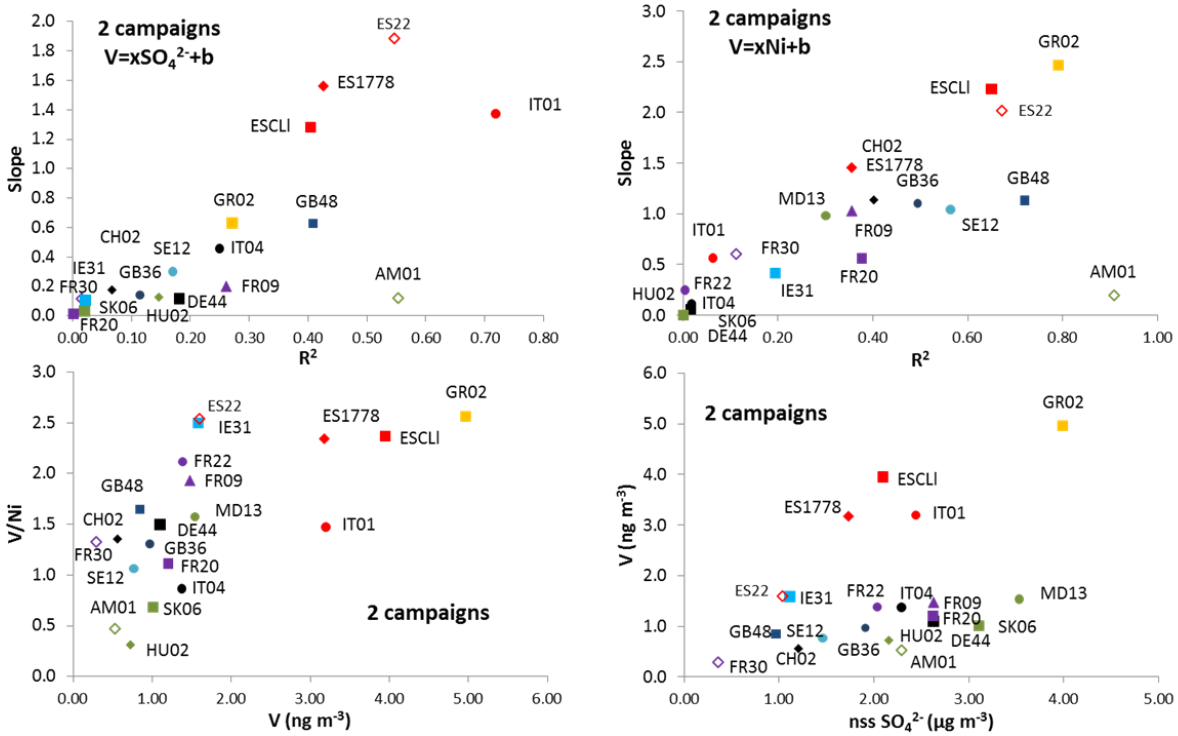

Figure S8: Scatter plots for: Top – determination coefficients (R^2) and the slopes (x) of the regression equations (V (ng m^{-3}) = xSO_4^{2-}(µg m^{-3}) +b, and V (ng m^{-3})= m Ni (ng m^{-3})) calculated at each site considering the two IMPs; Bottom - the ratio V/Ni with V concentrations and the averaged concentrations of V with SO_4^{2-}.

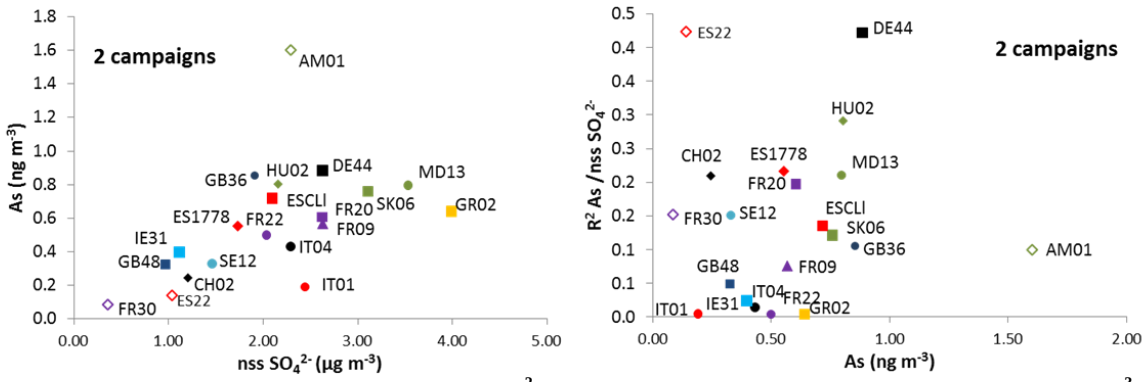

Figure S9: Scatter plots for correlation coefficients (R^2) and the slopes (x) of the regression equations (As (ng m^{-3})= xSO_4^{2-}(µg m^{-3}) +b), calculated at each site considering the two IMPs. Correlation of As concentrations with nssSO_4^{2-} and with the R^2 coefficients.

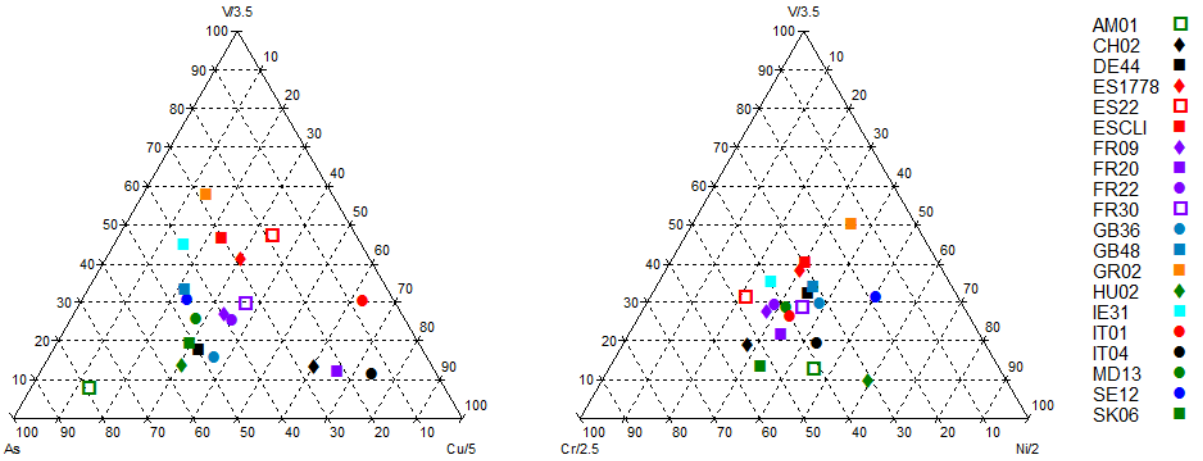

Figure S10: Ternary diagrams for traffic (Cu), fuel combustion (V/Ni), coal combustion (As) and industrial (metallurgy, Cr, Ni) trace metal tracers for NO-SDE sampling days during the EMEP IMPs.